Indian Journal of Pure & Applied Physics
Vol. 57, June 2019, pp. 422-426

Annealing temperature optimization for highly sensitive ZnO based acetone gas sensor

Manish Deshwal[a] & Anil Arora[b]*

[a]Electronics and Communication Engineering Department, Chandigarh University, Mohali 140 413, India

[b]Electronics and Communication Engineering Department, Thapar Institute of Engineering & Technology, Patiala 147 004, India

Received 19 April 2018; accepted 01 March 2019

The present research is related to the effect of temperature on the crystallinity for zinc oxide (ZnO) thin film based acetone sensor fabricated via sol-gel method. One of the critical parameters for a gas sensor is the annealing temperature of thin films which directly influences the crystallinity of a material and hence its structural properties. Thus, the present study shows the effects of annealing temperature variation over the properties related to the gas sensing behaviour for the sensor. The structural and optical properties with surface morphology have been analysed for the prepared samples. The response characteristics of the ZnO films with a thickness of 410 nm for the acetone vapour has been determined for the temperature range from 180 °C to 360 °C and the annealing temperature variation has been studied from 450 °C to 750 °C. The optimal operating temperature has been found to be 320 °C while the optimal annealing temperature as reflected by the results is 650 °C.

Keywords: Acetone sensor, Annealing temperature variations, Sol- Gel, ZnO

1 Introduction

Volatile organic compounds (VOC's) based sensors are significantly studied for various applications, such as monitoring air quality, breathing tests, environmental as well as health hazards, with many other industrial and scientific applications[1-8]. Acetone, a highly volatile organic solvent, is used in almost all fields either commercially or in the laboratories for various purposes like ultra-cleaning by removing organic residues up to nano level fabrications[9-11]. It is also used for detecting the level of acetone in breathing tests for diabetic patients[12]. Since there are several different kinds of acetone sensors depending on the specific applications[13-15]. There are various techniques that have been developed over the years for the fabrication of an acetone gas sensor with base sensing layer material as zinc oxide (ZnO)[15-23]. ZnO is a widely exploited material for its wide and direct band gap with semiconducting electrical properties, high exciton binding energy at room temperature, ease of fabrication and anisotropic crystalline structure[1,2]. Sol-gel is a very cost-effective method offering versatility for synthesizing one dimensional nano-structures having exceptional length, uniformity of diameter, and a high surface area[24-27]. In the present work, ZnO thin films has been studied for different annealing temperatures of 450 °C, 550 °C, 650 °C and 750 °C to optimize sensitivity, quick response and recovery times to acetone vapors with high selectivity.

As the crystallization of ZnO thin films depends upon the annealing temperature which leads to higher sensitivities for a gas sensor[28-30]. Hence, the following study presents a highly sensitive acetone sensor with an optimized annealing temperature with varying grain sizes and crystallinity. The optimum annealing temperature comes out to be 650 °C with a thickness[31] of 410 nm with a sensitivity of 63 for thermally volatized acetone vapors.

2 Experimental

ZnO thin films were synthesized using analytical grade reagents by Sigma-Aldrich. The precursor solution was prepared by dissolving zinc acetate dehydrate powder in ethanol maintaining 0.1 M molarity. Then monoethanolamine (MEA) was added as the stabilizing agent. The solution was stirred at 70 °C for 20 min in closed environment. The solution was left overnight for ageing. The pre-fabricated IDE patterned silicon wafers were used for the growth of ZnO thin films using spin coater at 3000 rpm for 15 s subsequently heating the prepared films at 300 ºC for 20 min (Fig. 1). The spin coating was performed

* Corresponding author (E-mail: anil.arora@thapar.edu)

recurrently to achieve the desired thickness of 410 nm. Then the prepared films for the sensors were annealed at various temperatures ranging from 450 °C to 750 °C individually for 6 hours. The characterization processes were carried out for the films deposited on the plane silicon wafer with IDE patterns with same parameters. The samples annealed at different temperatures 450 °C, 550 °C, 650 °C and 750 °C are encoded as S1, S2, S3 and S4 respectively. The characteristic studies for optical, structural and surface morphologies for the samples were carried out using UV-visible spectrophotometer, XRD and FESEM. An indigenously developed gas calibrator and test system (GCTS) consisting a glass bell jar, thermocouple, heating element, temperature controller and the contact pins connected to digital multimeter (DMM) Keithley 2002 is used for the data acquisition. Thermal volatization of liquid acetone is used for preparation of acetone vapours which are inserted in the chamber through calibrated leaks with desired concentration. The sensing response (S) is given by[32]:

$$S = \frac{R_g - R_a}{R_a} \quad \ldots(1)$$

Where R_a and R_g represent the resistances of the sensor in air and gas, respectively. The time taken to achieve 90% for the total resistance change for adsorption is termed as response time and for desorption, is termed as recovery time.

3 Results and Discussion

3.1 XRD analysis

Figure 2 represents the XRD patterns for the prepared ZnO thin films at distinctly annealed temperatures. The XRD graphs show the increasing profile of poly-crystallinity patterns for the samples viz. S1, S2, S3, S4.

As can be seen from Fig. 2 that all of the four samples indicate preferential orientation along c-axis. The peaks are identified to (100), (002), (101), (102), and (110) plane of reflections for a single phase wurtzite ZnO structure. The diffraction peaks in the XRD spectrum are matched with a pure hexagonal wurtzite structure (JCPDS No. 36-1451) for ZnO. For investigating the effects of annealing temperature variation over crystallinity patterns for the samples, the diffraction peaks (100), (002) and (101) are monitored. The calculations performed using Scherrer's relation from XRD graph is clearly indicating the increase in the crystallite size with the increase in annealing temperature of the ZnO layer as shown in Table 1. Hence, it can be concluded from the results that indicates the increasing atomic sizes with increase in annealing temperature from 450 °C to 750 °C. The improved crystal lattice structures and

Table 1 — Crystallite size variation with increasing annealing temperature.

Sample coding	Peak position 2θ (°)	FWHM B size (°)	*D*p (nm)	Dp average (nm)
S1	31.84637	0.36998	23.34	24.38
S2	34.90958	0.29178	29.83252219	26.54370443
S3	34.4437	0.1093	77.589123	43.74347683
S4	34.4433	0.1031	83.352807	47.246455

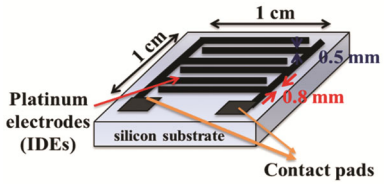

Fig. 1 — IDE schematic.

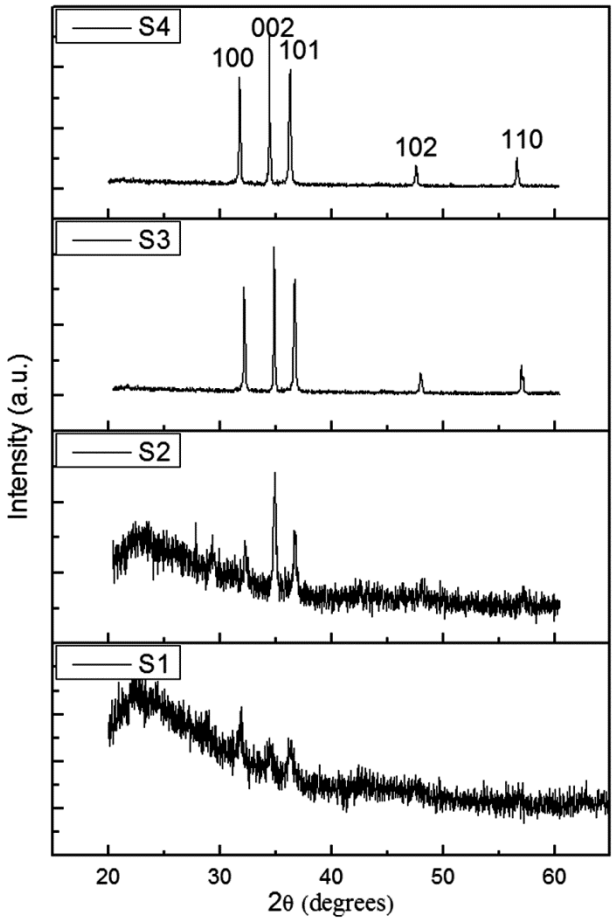

Fig. 2 — XRD patterns for S1, S2, S3 and S4.

the atomic sizes for the samples with increasing annealing temperatures can be directly related to adsorption and desorption phenomenon of the gas molecules over the surface of the thin films[28, 29].

3.2 Surface morphology

The structural characterizations are performed for the structural analysis of the prepared samples. Figure 3 shows the FESEM images of the ZnO thin film based sensor architecture. As shown in Fig. 3(a), S1 structure where the coagulated nanoparticles of ZnO over the sensor surface results in poor structural forms probably due to non-crystallinity or insufficient annealing temperature. Figure 3(b) presents the structure of S2, here it may be concluded that the sample S2 exhibits a better architecture but still a non-uniform less coagulated structures formed with much less surface to react with gas particles. Figure 3(c and d) shows the samples S3 and S4, respectively, which represents the ZnO nano-threads like structures are prepared with very high surface area to react with the gas molecules. Figure 3€ also represents a thickness of the sample of 410 nm. The FESEM images present clearly the changing crystallinity phases for all four samples.

3.3 Optical properties

Figure 4 shows the UV-visible transmittance spectra of ZnO thin films deposited on quartz substrates under similar deposition parameters. ZnO thin films are found to be highly transparent (~80%) in the visible region with adsorption edge at around 375 nm. The energy band gap (E_g) is calculated using Tauc plot (insets of Fig. 4) and is estimated to be in range for 4.3 eV to 3.7 eV. The energy band gap of ZnO decreases from 4.3 eV to 3.7 eV with the increase in annealing temperature[33]. The change in the values of transmittance as well as the band gaps clearly indicates the improving optical properties with increasing annealing temperature of the samples.

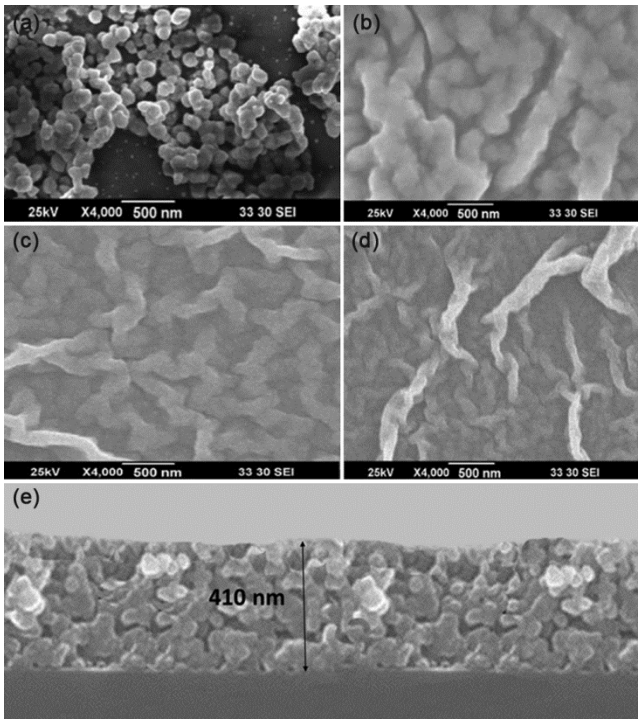

Fig. 3 — FESEM of (a) S1, (b) S2, (c) S3, (d) S4 and € cross sectional view of S3.

3.4 Gas sensing response

Before gas sensing, all the prepared sensors are annealed at 250 °C for 1 h for desorbing the surface of the samples for any gas contamination. Figure 5 shows the sensors responses for all the samples with temperature ranging from 180 °C to 360 °C. Figure 5 represents the sensors optimum operating temperatures in a closed environment with

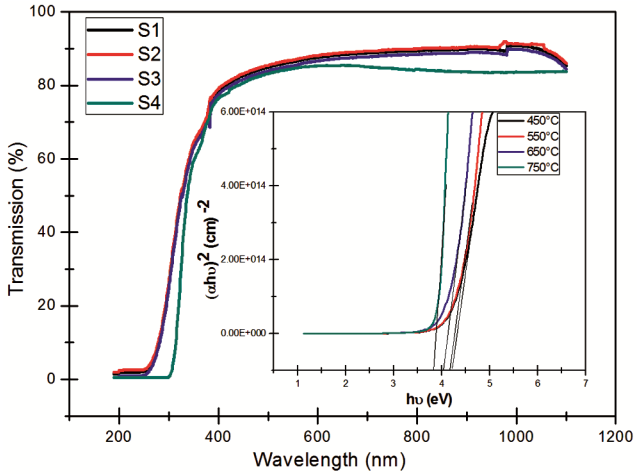

Fig. 4 — UV transmittance.

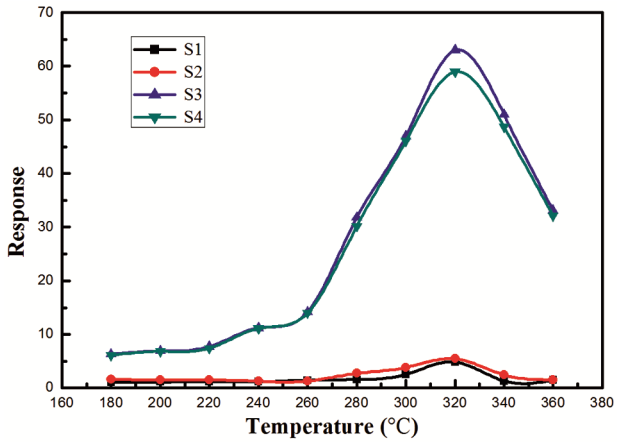

Fig. 5 — Sensor responses for sample S1, S2, S3 and S4.

concentration at 500 ppm of acetone vapors. The sensing response values for S1, S2, S3, and S4 increase evidently till maximum values at optimum operating temperatures, then the sensing responses degrades with increasing operating temperatures[30]. These results may be explained by kinetics and the gas sensing mechanisms over the ZnO thin film surfaces[23]. At lower operating temperatures the gas molecules kinetics is low following which results in lower sensing responses. Also at operating temperatures higher than the optimal operating temperature, the kinetics of gas molecules is that much large that molecules may escape from the active centers of the surface before reactions and will affect the quantity of the gas to be adsorbed. Hence, resulting in lower sensor response. As clearly seen from the Fig. 5, S3 and S4 exhibit the highest and somehow equal responses that may be due to the large surface interactions, oxygen vacancies, and open network architectures. The results also show the effect of crystallinity dependant sensing behaviors for the thin film samples where the higher crystallinity concludes for better sensitivity.

The higher annealing temperatures usually results in enhanced crystallinity due to recrystallization or densification of atomic structures which further leads to enhanced chemical species detection capabilities. This may be due to the oxide layers with inferior crystallinity which contains a higher number of conducting electrons due to more structural imperfections resulting in a lower degree of resistance modulation for electrons originating from the interaction of gaseous species over the thin film surface hence, resulting in degraded sensing responses. However in the case of metal oxide thin films with higher degree of crystallinity, the number of carriers available will be lesser, which results in a more pronounced modulation of resistance caused by the adsorption and desorption of the gas molecules. Hence, better sensing responses are attained[28,29]. Figure 6 shows the sensing response of the sample S3 (with the highest sensitivity) with concentrations ranging from 50 ppm to 500 ppm at 320 °C optimal operating temperature.

Now, it may be concluded that the samples with higher annealing temperatures which in turn makes the sample highly crystalline exhibits higher and stable responses with nearly equal optimal operating temperatures. Figure 7 shows the response time and Fig. 8 presents the recovery times for all the four samples giving another important relation between the samples which depicts the decrease in response times and recovery times of the samples which are annealed

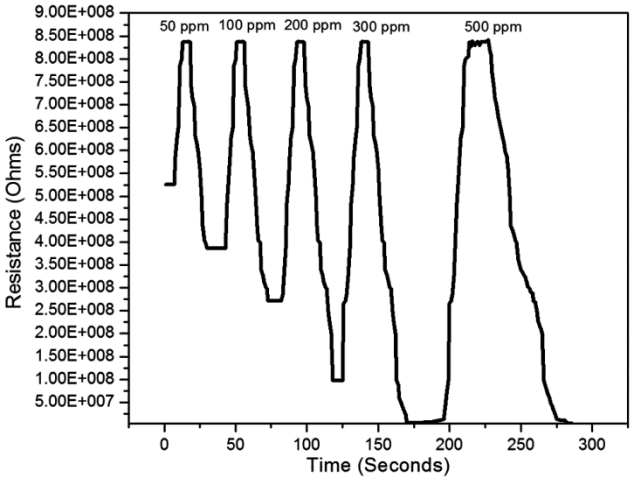

Fig. 6 — Response at various concentrations.

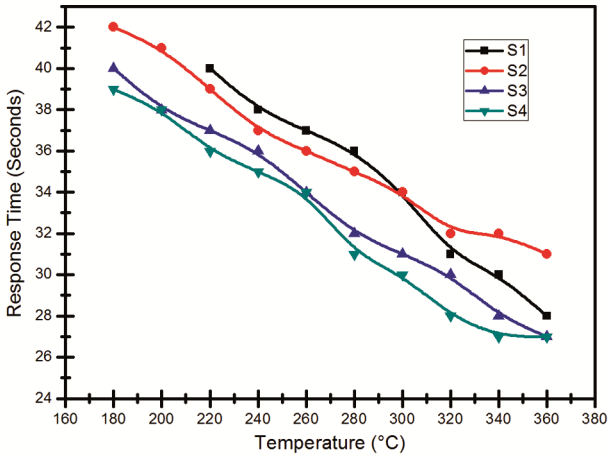

Fig. 7 — Response time versus temperature.

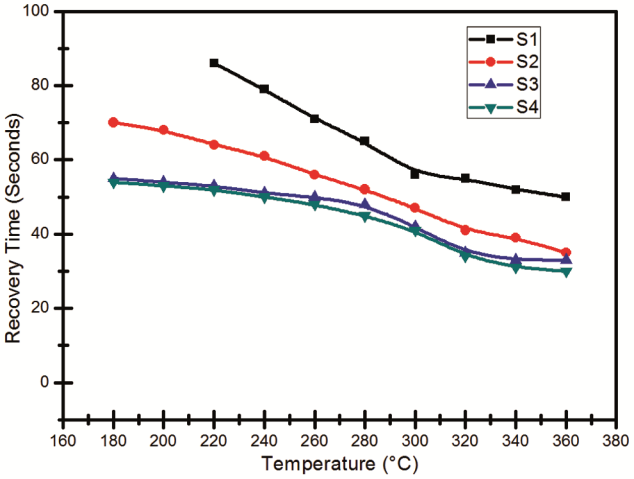

Fig. 8 — Recovery time versus temperature.

at higher temperatures. Also with the increasing operating temperatures, the response times and recovery times decrease for all the four sensors which relate to the higher rates of adsorption and desorption at high operating temperatures as discussed earlier.

4 Conclusions

The acetone sensing characteristics were studied for ZnO thin film sensors with variation in annealing temperature. Samples with higher annealing temperatures showed enhanced response over the samples with lower annealing temperatures. The results clearly indicate towards crystallinity-dominant domains that represent the enhanced crystallinity for the crystal structures which plays crucial roles in sensing mechanisms. In contrast at higher annealing temperatures, the effect of grain growth proves to be a crucial parameter as marginal enhancement of the crystallinity with increased atomic structures degrades the sensing capabilities of the sensor. The results suggested for attentive observations to optimize the size and crystallinity of the atomic structures simultaneously to attain superior sensing capabilities. This may also be concluded that the variations in annealing temperatures do not affect optimal operating temperature for a gas sensor.

Acknowledgement

Authors are thankful to Prof Vinay Gupta, Department of Physics and Astrophysics, University of Delhi for providing the access to laboratory equipment for carrying out experimental work and characterization.

References

1 Arora A, Arora A, George P, Dwivedi V & Gupta V, *Sens Transducers*, 117 (2010) 92.
2 Arora A, Arora A, Dwivedi V, George P, Sreenivas K & Gupta V, *Sens Actuators A: Phys*, 141 (2008) 256.
3 Zhu B, Xie C, Wang W, Huang K & Hu J, *Mater Lett*, 58 (2004) 624.
4 Yoon J, Chae S K & Kim J M, *J Am Chem Soc*, 129 (2007) 3038.
5 Srivastava A, *Sens Actuators B: Chem*, 96 (2003) 24.
6 Wen Z & Tian M L, *Phys B: Condensed Matter*, 405 (2010) 1345.
7 Janzen M C, Ponder J B, Bailey D P, Ingison C K & Suslick K S, *Anal Chem*, 78 (2006) 3591.
8 Lee D S, Kim Y T, Huh J S & Lee D D, *Thin Solid Films*, 416 (2002) 271.
9 Chiao J S & Sun Z H, *J Mol Microbiol Biotechnol*, 13 (2007) 12.
10 Ni Y & Sun Z, *Appl Microbiol Biotechnol*, 83 (2009) 415.
11 Deshwal M & Arora A, *J Mater Sci: Mater Electron*, (2018) 1.
12 Phillips M, *Anal Biochem*, 247 (1997) 272.
13 Shan H, Liu C, Liu L, Li S, Wang L & Zhang X, *Sens Actuators B: Chem*, 184 (2013) 243.
14 Phanichphant S, Liewhiran C, Wetchakun K, Wisitsoraat A & Tuantranont A, *Sensors*, 11 (2011) 472.
15 Li X, Ma S, Li F, Chen Y, Zhang Q & Yang X, *Mater Lett*, 100 (2013) 119.
16 Qi Q, Zhang T, Liu L, Zheng X, Yu Q & Zeng Y, *Sens Actuators B: Chem*, 134 (2008) 166.
17 Anno Y, Maekawa T, Tamaki J, Asano Y, Hayashi K & Miura N, *Sens Actuators B: Chem*, 25 (1995) 623.
18 Zeng Y, Zhang T, Yuan M, Kang M, Lu G, Wang R, *Sens Actuators B: Chem*, 143 (2009) 93.
19 Shen W, Zhao Y & Zhang C, *Thin Solid Films*, 483 (2005) 382.
20 Wei S, Zhou M & Du W, *Sens Actuators B: Chem,* 160 (2011) 753.
21 Ge C, Xie C & Cai S, *Mater Sci Eng B*, 137(2007) 53.
22 Liu L, Li S, Zhuang J, Wang L, Zhang J & Li H, *Sens Actuators B: Chem,* 155 (2011) 782.
23 Wang J, Sun X, Yang Y, Huang H, Lee Y & Tan O, *Nanotechnology*, 17 (2006) 4995.
24 Lee J H, Ko K H & Park B O, *J Crystal Growth,* 247 (2003) 119.
25 Lee J H & Park B O, *Thin Solid Films*, 426 (2003) 94.
26 Lin K F, Cheng H M, Hsu H C, Lin L J & Hsieh W F, *Chem Phys Lett*, 409 (2005) 208.
27 Musat V, Teixeira B, Fortunato E, Monteiro R & Vilarinho P, *Surf Coat Technol*, 180 (2004) 659.
28 Katoch A, Sun G J, Choi S W, Byun J H & Kim S S, *Sens Actuators B: Chem,* 185 (2013) 411.
29 Katoch A, Abideen Z U, Kim J H & Kim S S, *Metal Mater Int,* 22 (2016) 942.
30 Seeley Z M, Bandyopadhyay A & Bose S, *Mater Sci Eng B*, 164 (2009) 38.
31 Kakati N, Jee S H, Kim S H, Oh J Y & Yoon Y S, *Thin Solid Films*, 519 (2010) 494.
32 Tyagi P, Sharma A, Tomar M & Gupta V, *Sens Actuators B: Chem*, 224 (2016) 282.
33 Johnson E, Prod'homme P, Boniface C, Huet K, Emeraud T & Cabarrocas P R, *Sol Energy Mater Sol Cells*, 95 (2011) 2823.